

# Green Synthesis of Tannic Acid-Mediated Chromium Oxide Nanocomposites using *Acalypha Indica* and *Carica Papaya* Leaf and its Biomedical Applications

Sulochana Govindharaj<sup>1</sup>, Abin Mahmood Nizar<sup>2</sup>, Akilaa O B<sup>1</sup>,  
Rajeshkumar Shanmugam<sup>1\*</sup>, Lakshmi Thangavelu<sup>3</sup>

<sup>1</sup>Nanobiomedicine Lab, Centre for Global Health Research, Saveetha Medical College and Hospital, Saveetha Institute of Medical and Technical Sciences, Tamil Nadu, India

<sup>2</sup>Department of Orthopaedics, Saveetha Medical College and Hospital, Saveetha Institute of Medical and Technical Sciences, Chennai, India

<sup>3</sup>Centre for Global Health Research, Saveetha Medical College and Hospital, Saveetha Institute of Medical and Technical Sciences, Tamil Nadu, India

Email: [rajeshkumars.smc@saveetha.com](mailto:rajeshkumars.smc@saveetha.com)

Nanotechnology produces nanosized particles with unique physicochemical properties that combine science and technology. Chromium oxide nanoparticles ( $\text{Cr}_2\text{O}_3$  NPs) are transition metal oxide particles that have extensive applications in different fields. *Acalypha indica* and *Carica papaya* are two plants that are known for their medicinal properties, and tannic acid which has natural antioxidant properties has also been utilised in traditional medication to treat many ailments. To study the biosynthesis of chromium oxide nanoparticles using *Acalypha indica* & *Carica papaya* incorporated with tannic acid and their potential biomedical applications. The  $\text{Cr}_2\text{O}_3$  nanoparticles were biologically synthesised with *Acalypha indica* and *Carica papaya* leaf extract using chromium sulphate as a precursor. The synthesized nanoparticles were treated with tannic acid to make them a tannic acid-mediated chromium oxide nanocomposite (TA- $\text{Cr}_2\text{O}_3$  NC). The prepared TA- $\text{Cr}_2\text{O}_3$  NCs were characterised using UV-VIS and XRD techniques and their antibacterial, antioxidant, anti-inflammatory, anticoagulant, and cytotoxicity activities were assessed at different concentrations. The TA- $\text{Cr}_2\text{O}_3$  nanocomposites were successfully synthesized and the SPR absorbance peak was obtained at 360 nanometers at 24 hours. The antibacterial activity results show that *Pseudomonas* sp. was more susceptible to TA- $\text{Cr}_2\text{O}_3$  NCs. Other activity results also tell us the exceptional anti-inflammatory, antioxidant, and cytotoxicity properties of TA- $\text{Cr}_2\text{O}_3$  NCs. Nanosized TA- $\text{Cr}_2\text{O}_3$  NCs showed effective properties against all tested activities. Due to their low manufacturing cost and high effectiveness in biomedical properties, TA- $\text{Cr}_2\text{O}_3$  NCs may find wide applications in various fields.

**Keywords:** *Acalypha indica*, Biomedical applications, *Carica papaya*, Chromium oxide nanoparticles, Tannic acid.

## 1. Introduction

Nanotechnology is the field that combines both science and technology and uses commercially prepared nanosized particles which are one billionth of a metre with various unique physicochemical properties (Sahu et al., 2021). In the past decade, nanomedicine has been an excellent area that aims to improve the quality of healthcare strategies and is widely used for catalysis, ecology, engineering and therapeutic purposes (Shabatina et al., 2020). Magnetic nanoparticles exhibit magnetic properties due to the motion or spin of the electrons of an atom (Ying et al., 2022). The characteristics of magnetic nanoparticles (MNPs) are influenced by factors such as their size, shape, crystalline structure, magnetization, and chemical composition. In the presence of a magnetic field, MNPs act like small permanent magnets, often forming lattice networks or large aggregates. However, their magnetism diminishes once the magnetic field is removed. MNPs offer diverse functionalities in biomedical applications, including magnetic resonance imaging, controlled release systems, catalysis, bioseparation, drug delivery, biosensors, data storage, magnetofection, and hyperthermia, and exhibit excellent biocompatibility, making them highly appealing in the biomedical field (Çetin et al., 2019). Chromium oxide nanoparticles ( $\text{Cr}_2\text{O}_3$ NPs) possess distinctive optical attributes, making them valuable in diverse applications including catalysis (Mori et al., 2017), photocatalysis (Zelekew et al., 2021), solar energy collection, lithium-ion batteries (Zhu et al., 2012), energy storage, thermal protection, liquid crystal displays, and various applications in biomedicine such as drug delivery (Azizi, 2020). They exhibit excellent melting point, hardness, stability, and high resistivity with a 3.4 eV wide bandgap (Iqbal et al., 2020). Additionally, they have shown promise in medical applications, serving as antioxidants, anti-cancer agents, antiviral compounds, antibacterial agents, and anti-diabetic agents (Zainab et al., 2022). Characterisation methods including transmission electron microscopy and X-ray diffraction have confirmed the rhombohedral polycrystalline nature of chromium oxide nanoparticles (Isacfranklin et al., 2020). There are three different types of synthesis procedures for chromium oxide nanoparticles that include chemical, physical and biological synthesis. As we all know, the  $\text{Cr}_2\text{O}_3$  nanoparticles that are prepared by conventional methods like chemical or physical exhibit several disadvantages by using various hazardous chemicals that impart additional environmental toxicity and carcinogenicity of the nanoparticles (Bahrulolum et al., 2021). Thus, the green synthesis of nanoparticles has developed as an alternative to conventional physical and chemical methods as it is cost-effective, straight forward, and eco-friendly. Green synthesis is a fascinating process that uses parts of plants, bacteria, and fungi to produce nanoparticles which are found to be cancer-fighting cytotoxic agents. Compared to bacteria and fungi, plant extract synthesis of nanoparticles is very simple and gives an uncomplicated approach to producing nanoparticles on a large scale. For this experimental work, a biogenic procedure was used to synthesise chromium oxide nanoparticles using *Acalypha indica* and *Carica papaya* plant leaf extracts. *Acalypha indica*, also known as Indian acalypha, is a weed that is commonly found in Sri Lanka, India, tropical Africa, Pakistan, and many other countries. This weed has been used in traditional Sri Lankan and Indian medicine to treat various ailments like bronchial asthma, constipation, skin disorders, and snake bites, among others (Perera & Teklani, 2016).

The plant is also suitable for use as a low-cost vegetable as it has a high moisture content (>90%) and a high ash value (>18%). It is also rich in various minerals, with iron being the

most abundant, followed by copper, zinc, and other micro-elements. Some of the most promising health benefits of this plant include its potential to act as an anticancer, analgesic, anti-inflammatory, antifungal, anthelmintic, antibacterial, antiviral, anti-diabetes, antioxidant, antiulcer (Kalimuthu et al., 2010), anti-ageing, anti-hyperlipidemic, anti-hemolytic, anti-obesity (Naik et al., 2019), anti-venom, and hepatoprotective agent (Girija et al., 2018; Wang et al., 2017). Carica papaya leaf extract has been used as a traditional medicine by ancient humans to treat infectious diseases such as malaria, dengue, and chikungunya. Papaya is a plant that belongs to the family Caricaceae and is known worldwide for its therapeutic and nutritional properties. Papaya leaves have been used to treat fever, asthma, colic, beriberi, jaundice, and other ailments (Krishna et al., 2008). The papaya plant is a rich source of vitamins A, B, and C and a good source of calcium and iron (Wall, 2006). The enzyme papain, found in papaya, aids in digestion and can be used to treat ulcers and some microbial diseases, particularly gram-negative bacteria at higher doses (Leader et al., 2008). Papaya leaves contain carbohydrates, vitamins, lipids, and proteins, making them a nutritious food source. The compounds found in papaya leaves, including ascorbic acid (38.6%), protein (5.6%), phosphoric acid (0.225%), carbohydrates (8.3%), iron (0.0064%), and minerals like magnesium (0.035%), vary in concentration (Saran & Choudhary, 2013). Quantitative phytochemical analysis has revealed the presence of 0.001% tannins, 0.022% saponins, 0.013% flavonoids, 0.011% phenolics, 0.019% alkaloids, and 0.004% steroids in aqueous PLE. Due to the presence of rich sources of phytochemicals, minerals, and vitamins, papaya leaf extract (PLE) has extraordinary medicinal properties that have been used to treat various human diseases and help prevent diseases since ancient times (Singh et al., 2020). These properties of plant extracts can be uplifted by adding tannic acid which acts as a stabilising and reducing agent for chromium oxide nanoparticles. Tannic acid is an antioxidant polyphenol that is naturally extracted from oak tree galls and is a main component in leather tanning, red wines, and iron gall ink. It is also used as a traditional medicine to treat various diseases. These tannic acids have also been discovered by our ancestors and it has recently gained attention in the field of biomedical research because of their antioxidant, anti-inflammatory, antiviral, antifungal, anticancer and antibacterial properties (Yemmen et al., 2017; Ahmad, 2014). Tannic acid can also be used in developing thin films, hydrogels and nanoparticles for wound healing, drug delivery and tissue regeneration. At certain concentrations, TA can trigger the cell metabolism of bacteria & viruses leading to apoptosis by interfering with essential proteins (Baldwin & Booth, 2022). Because of this property, in this research experiment, tannic acid is incorporated into the prepared chromium oxide nanoparticles biosynthesized from the plant extract of *Acalypha indica* and *Carica papaya* and is used to evaluate antimicrobial, anti-inflammatory, antioxidant, and cytotoxicity studies.

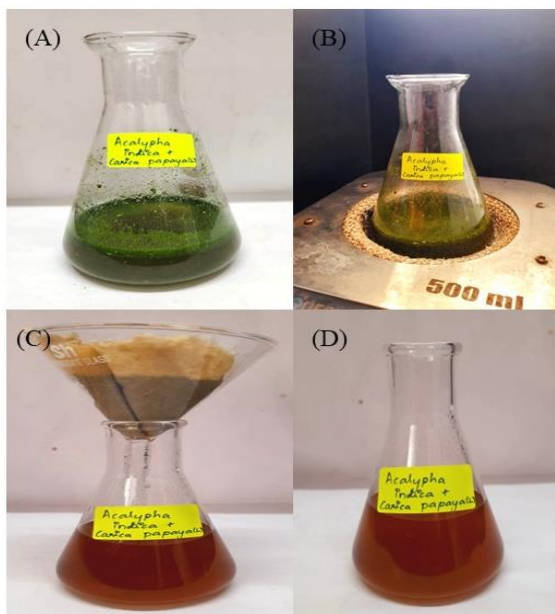
## **2. Materials and Methods**

### **2.1. Extraction of plant material**

Fresh leaves of *Acalypha indica* and *Carica papaya* were obtained from a garden, and they were thoroughly washed twice using running water. After that, they were dried under the shade of the sun at 37° to 40°C temperature. The dried leaves were then crushed and turned into powder form. An accurate measurement of 1 g of each *Acalypha indica* and *Carica papaya*

leaf powder was added to 100 ml of distilled water (Figure 1A). The mixture was heated to 50°C and boiled for 15-20 minutes to activate the phytochemicals present in the plant extract (Figure 1B). The extract was then filtered using a muslin cloth (Figure 1C & 1D) and stored at low temperatures for further use.

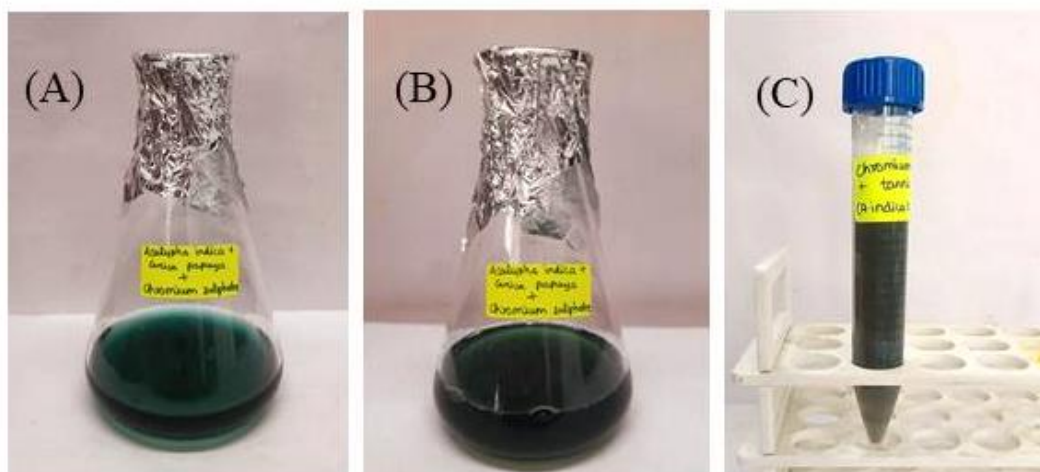
Figure 1. Preparation of plant extract - *Acalypha indica* & *Carica papaya*



## 2.2. Biosynthesis of $\text{Cr}_2\text{O}_3$ NPs mediated tannic acid ( $\text{TA-Cr}_2\text{O}_3$ )

A measured quantity of 40 ml of the prepared plant extract was added to 60 ml of 20 mM of Chromium sulphate solution (Figure 2A). The prepared nanoparticle solution is kept in the orbital shaker for 24 hours (Figure 2B). The 5 ml pellet was collected by centrifugation at 8,000 rpm for 10 min (Figure 3). Then 100 mg of tannic acid is dissolved in 1 ml of distilled water. This mixture is then added to 4 ml chromium oxide nanoparticle solution which we prepared before. The tannic acid-mediated chromium oxide nanocomposites were collected and stored in the refrigerator for further use (Figure 2C, 5).

Figure 2. (A) Precursor solution (Chromium sulphate solution) (B) Preparation of chromium oxide nanoparticle solution (C) Preparation of tannic acid-mediated chromium oxide nanocomposite (TA-Cr<sub>2</sub>O<sub>3</sub> NCs)



### 2.3. Characterisation of chromium oxide NPs

UV-Vis spectroscopy is a widely used technique to characterize nanoparticles based on their size, shape, and distribution. This method is used to determine the surface plasmon resonance (SPR) or absorbance peak of the fabricated nanoparticle, which is essential for determining the absorption of liquids and other compounds. For Cr<sub>2</sub>O<sub>3</sub> NPs, the SPR falls within the range of 250–650 nm. It has been found that the type of extract, temperature, pH, and route of manufacturing can affect the SPR of Cr<sub>2</sub>O<sub>3</sub> NPs, which in turn affects their morphological properties (Ghotekar et al., 2021). The colour change of the solution is a preliminary confirmation study for the formation of chromium oxide nanoparticles. The unique optical properties of these nanoparticles usually exhibit a greenish-blue colour, which is dependent on their size and shape. The colour changes occur due to the effect of SPR on the nanoparticles. This analysis technique provides important details about the size, stability, structure, and agglomeration of Cr<sub>2</sub>O<sub>3</sub> NPs (Kanniah et al., 2020). The UV absorbance peak of chromium oxide nanoparticles and tannic acid-mediated chromium oxide nanocomposites was measured using a UV-visible spectrophotometer every 1 hr, 12 hr, 24 hr, 36 hr and 48 hours at 250 nm to 650 nm.

### 2.4. Antibacterial activity of TA-Cr<sub>2</sub>O<sub>3</sub> NCs

The agar well diffusion technique assessed the antibacterial activity of the green synthesised tannic acid-mediated chromium oxide nanocomposites. Mueller Hinton agar plates were made and autoclaved for 15–20 minutes at 121°C to achieve sterility. The bacterial cultures such as *Staphylococcus aureus*, *Pseudomonas aeruginosa*, *Escherichia coli*, and *Enterococcus faecalis* were prepared and were equally dispersed across the agar plate using sterile cotton swabs. In the agar plates, wells of 9 mm in diameter were made using a sterile polystyrene tip. Various concentrations of TA-Cr<sub>2</sub>O<sub>3</sub> NCs (25 µg/ml, 50 µg/ml, and 100 µg/ml) along with standard (Amoxyrite antibiotic) were added to the wells. The plates were incubated at 37°C for 24 hours

*Nanotechnology Perceptions* Vol. 20 No. S7 (2024)

and 48 hours and the zone of inhibition was calculated.

#### 2.4.1. Time kill curve assay

A 1 ml aliquot of the bacterial suspension (*Staphylococcus aureus*, *Pseudomonas aeruginosa*, *Escherichia coli*, and *Enterococcus faecalis*) was added to 9 ml of Muller Hinton broth containing the TA- Cr<sub>2</sub>O<sub>3</sub> NCs at a concentration of 25, 50 and 100 µg/ml. The final microbial concentration was approximately 10<sup>6</sup> CFU/mL. The mixture was then incubated at 37° C with shaking at 200 rpm for varied time intervals (0,4,6,8,10,12 & 24 hr). Then the percentage of dead cells is calculated at a wavelength of 600 nm at regular time intervals.

### 2.5 Antioxidant activity

Multiple assays such as 2,2-diphenyl-1-picrylhydrazyl (DPPH), Hydrogen peroxide assay, 2,2-azino-bis-3-ethylbenzothiazoline-6-sulphonic acid (ABTS), Ferric reducing antioxidant power (FRAP), and Nitric oxide assay were used to determine the antioxidant nature of Tannic acid mediated chromium oxide nanocomposites (TA-Cr<sub>2</sub>O<sub>3</sub> NCs).

#### 2.5.1. DPPH assay

A methanol-based stock solution of 0.1mM 2,2-diphenyl-1-picrylhydrazyl (DPPH) was prepared. For every assay, a fresh working solution was made by diluting the stock solution to a final concentration of 20 µM in methanol. 1 ml of the working solution was added into 5 test tubes with different concentrations (10, 20, 30, 40, 50 µg/mL) of TA-Cr<sub>2</sub>O<sub>3</sub> NCs. Ascorbic acid was used as the standard. The test tubes were incubated for 15 minutes in dark conditions. After the incubation period, these mixtures were added to the 96-well plate and the absorbance was measured at 517 nm.

#### 2.5.2. Hydrogen peroxide assay

The antioxidant activity of TA-Cr<sub>2</sub>O<sub>3</sub> NCs was assessed using the Hydrogen peroxide assay (H<sub>2</sub>O<sub>2</sub>). Five test tubes were taken, and 1 ml of H<sub>2</sub>O<sub>2</sub> was added to each tube. TA-Cr<sub>2</sub>O<sub>3</sub> NCs with concentrations of 10, 20, 30, 40, and 50 µg/ml were added to each tube. The sample mixture was then incubated in a dark place for 10 minutes. After incubation, the mixtures were transferred to a 96-well plate at a concentration of 200 µl. The absorbance of the mixture was measured at 532 nm.

#### 2.5.3. FRAP assay

3.1 g of sodium acetate trihydrate was weighed, and then 16 ml of glacial acetic acid was added to bring the volume up to 1 litre, followed by the addition of distilled water, resulting in the preparation of the acetate buffer. Next, a solution of 10 millimolar TPTZ (2,4,6-tripyridyl-s-triazine) was mixed with 40 millimolar HCl, and a solution of 20 millimolar FeCl<sub>3</sub>.6H<sub>2</sub>O was prepared. These solutions were combined in a ratio of 10:1:1 to create the FRAP reagent. 3.6 ml of the FRAP solution was mixed with 0.4 ml of distilled water and placed in an incubator at 37°C for 10 minutes. TA-Cr<sub>2</sub>O<sub>3</sub> NCs were added to the solution at five different concentrations (10, 20, 30, 40 & 50 µg/ml) and incubated at 37°C for 10 minutes. The absorbance of the reaction mixture was measured at 593 nm.

#### 2.5.4. Nitric oxide radical inhibition assay

The nitric oxide radical inhibition can be determined through the Griess Illosvoy reaction, as *Nanotechnology Perceptions* Vol. 20 No. S7 (2024)



proposed by Garrat in 1964. A modification was made to the Griess Illosvoy reagent by substituting it with naphthyl ethylenediamine dihydrochloride (0.1% w/v). The reaction mixture, consisting of sodium nitroprusside (10mm, 2mL), phosphate buffer saline (0.5mL), and TA-Cr<sub>2</sub>O<sub>3</sub> NCs in different concentrations (10 µg to 50 µg) was added in five test tubes and incubated at 25°C for 150 minutes. After the incubation period, 0.5mL of each reaction mixture was mixed with sulfanilic acid reagent (1mL), and the solution was left undisturbed for 5 minutes to allow for complete diazotization. Next, 1mL of naphthyl ethylenediamine dihydrochloride was added, mixed, and allowed to stand for 30 minutes at 25°C. In diffused light, a pink-coloured chromophore is formed. The corresponding blank solutions were used to measure the absorbance of the solutions at 540 nm.

#### 2.5.5. ABTS assay

ABTS radical cation was formed through a reaction between 7.0 mM ABTS (diluted in 50% ethanol) and 2.45 mM potassium persulfate (diluted in distilled water). The reagent was then refrigerated for 24 hours. Before use, the reagent was diluted with 50% ethanol until it reached an absorbance of 1.0 at 734 nm. In a 96-well microplate, 250 µl of ABTS radical cation and 20 µl of TA-Cr<sub>2</sub>O<sub>3</sub> NCs (in concentrations of 10, 20, 30, 40 & 50 µg/mL) were added. The mixture was incubated in dark conditions for 10 minutes. After incubation, the reading was taken at 734 nm.

The antioxidant radical scavenging activity (%) was calculated by the equation,

$$\% \text{ Radical scavenging activity} = \frac{\text{Absorbance of control} - \text{Absorbance of sample}}{\text{Absorbance of control}} \times 100$$

#### 2.6. Anti-inflammatory activity

##### 2.6.1. Egg albumin assay

To perform, the egg albumin denaturation assay, 0.2 ml of fresh egg albumin was mixed with 2.8 ml of phosphate buffer (1x). Different concentrations (10-50 µg/ mL) of tannic acid-mediated chromium oxide nanocomposites were added to the reaction mixture. The pH was adjusted to 6.3. Then it was kept at room temperature for 10 minutes followed by incubation in the water bath at 55°C in a water bath for 30 min. Diclofenac sodium was used as the standard group while dimethyl sulphoxide was used as control. Then, the samples were measured spectrophotometrically at 660nm.

The percentage of protein denaturation was determined utilizing the following equation,

$$\% \text{ inhibition} = \frac{\text{Absorbance of control} - \text{Absorbance of sample}}{\text{Absorbance of control}} \times 100$$

##### 2.6.2. Membrane stabilisation assay

The in vitro heat-induced membrane stabilization assay is a widely used technique for evaluating the membrane stabilizing properties of natural and synthetic compounds. This assay measures the ability of a compound to stabilize the cell membrane by preventing its disruption and subsequent release of intracellular contents. To prepare RBC suspension, Collect fresh human blood in a sterile tube containing an anticoagulant. Centrifuge the blood at 3000 g for 10 minutes at room temperature to separate the RBCs from other blood components. Remove the supernatant and wash the RBCs three times with PBS. Resuspend the RBCs in the saline

and store them at 4°C to obtain a 10% (v/v) RBC suspension. Pipette 1mL of the RBC suspension into each centrifuge tube. Then different concentrations (10, 20, 30, 40 & 50 µg/mL) of tannic acid-mediated chromium oxide nanocomposites were added to each tube. Mix gently and incubate the tubes at 56°C for 30 minutes. Centrifuge the tubes at 2500 g for 5 minutes at room temperature to pellet the RBCs. Measure the absorbance of the supernatant at 560 nm using a UV-Vis spectrophotometer.

#### 2.6.3. Bovine serum assay

Firstly, 0.05 g of commercial bovine serum albumin was dissolved in 50 ml of distilled water. In each of the five test tubes, 3 ml of the solution was added. TA-Cr<sub>2</sub>O<sub>3</sub> NCs were added in varying concentrations to each test tube. After a 10-minute incubation, the test tubes were placed in a 50°C-water bath. Next, 200 µl of the sample mixture was added to a 96-well plate. Finally, the absorbance of the sample mixtures was analysed at 660 nm.

The percentage of protein denaturation was determined utilizing the following equation,

$$\% \text{ inhibition} = \frac{\text{Absorbance of control} - \text{Absorbance of sample}}{\text{Absorbance of control}} \times 100$$

#### 2.7. Anticoagulant activity

The anticoagulant activity of the TA-Cr<sub>2</sub>O<sub>3</sub> nanocomposites was evaluated on freshly collected human blood at room temperature. In this study, 1 mL suspension of tannic acid-mediated chromium oxide nanocomposites (concentration 50 µg/mL) was added to 10 mL fresh human blood. Another 10 mL of blood without addition was taken as a control. The two blood samples were then observed for the next 1 h at room temperature for any noticeable changes.

#### 2.8. Cytotoxic activity

The cytotoxicity activity of tannic acid-mediated chromium oxide nanocomposites (TA-Cr<sub>2</sub>O<sub>3</sub>) was examined using brine shrimp lethality assay.

##### 2.8.1. Brine shrimp lethality assay

The Brine shrimp larvicidal assay (BSLA) was used to evaluate the cytotoxicity of TA-Cr<sub>2</sub>O<sub>3</sub> NCs. To culture the Brine shrimp eggs, saltwater was prepared. A mixture of 2 g iodine-free salt and 200 ml of distilled water was used. 10 to 12 mL of prepared saltwater was poured into a 6-well ELISA plate. Nauplii of the shrimp were collected after 24 hours and 10 Nauplii were added to each well of the 6-well ELISA plate. TA-Cr<sub>2</sub>O<sub>3</sub> NCs in varying concentrations of 5, 10, 20, 40, and 80 µg/mL were added to each well, and one well was used as a control. The plates were incubated for 24 hours. After 24 hours, the survival of the nauplii was assessed and calculated using the following formula,

$$\% \text{ Cytotoxicity} = \frac{\text{Number of dead nauplii}}{\text{Number of dead nauplii} + \text{number of live nauplii}} \times 100$$

### 3. Results

#### 3.1. UV-visible spectroscopy

Visible colour changes from light green to darkish green begin after the addition of Acalypha



indica and Carica papaya plant extract to the chromium sulphate precursor solution after hours of incubation in an orbital shaker and it typically reveals the formation of chromium oxide nanoparticles. The SPR peak was monitored from 250-650 nm and the peak was centred at 410 nm after 48 hours (Figure 4).

Figure 3. (A) Day 1 observation of *Acalypha indica* + *Carica papaya*-mediated chromium sulphate solution was seen (B) darker greenish colouration of nanoparticle solution is observed at 48 hours which interprets the formation of chromium oxide nanoparticles

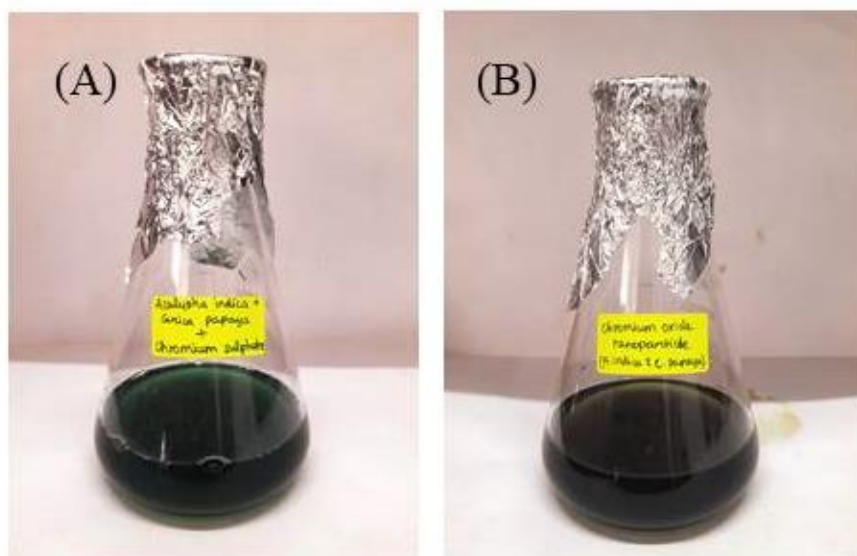
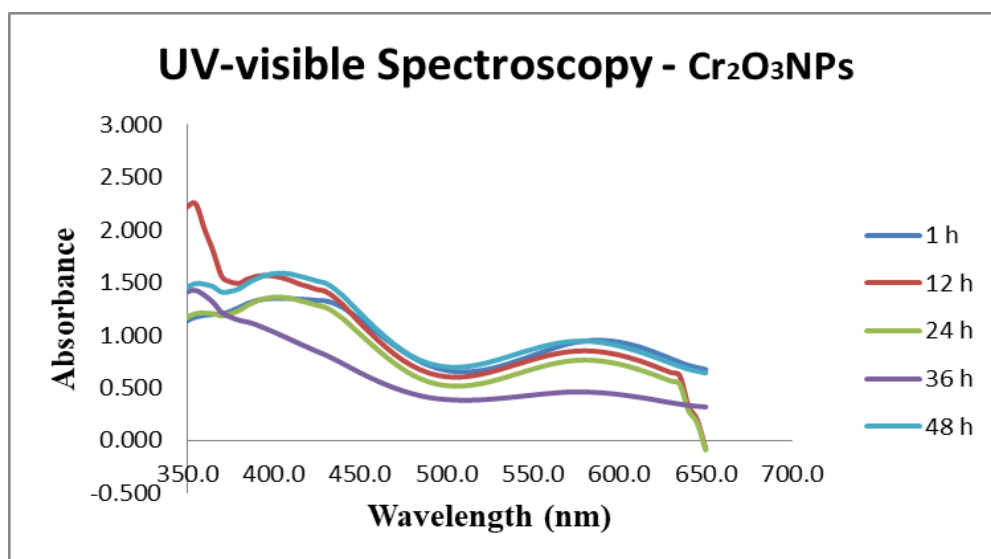


Figure 4. UV-visible spectroscopy graph of CrO NPs taken in various hour intervals



The addition of tannic acid to chromium oxide nanoparticles makes TA-Cr<sub>2</sub>O<sub>3</sub> nanocomposite which is shown in Figure 10. The UV-visible spectra absorbance peak was confirmed at the wavelength of 360 nm at 24 hours (Figure 6). The colour change was observed and its structure & crystallography were studied by assessing XRD. The mean crystalline sizes of TA-Cr<sub>2</sub>O<sub>3</sub> NC are calculated using Scherrer's equation.

Figure 5. Tannic acid-mediated chromium oxide nanocomposite

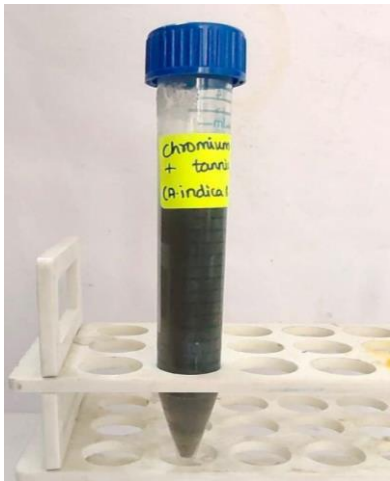
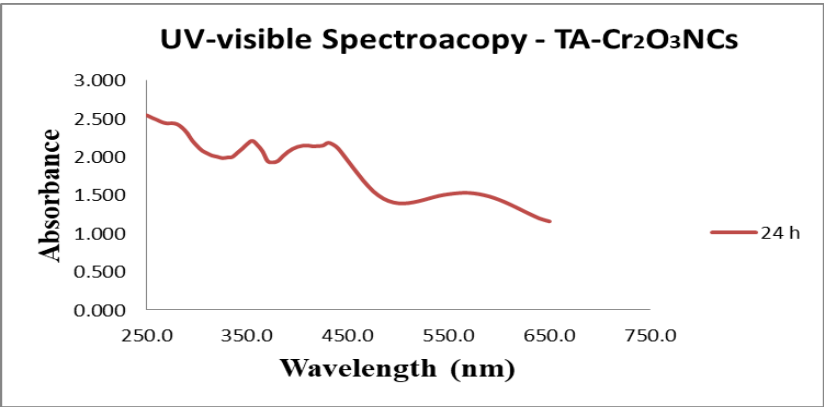


Figure 6. UV-visible spectroscopy graph of TA-Cr<sub>2</sub>O<sub>3</sub> NC taken in 24h



3.2. Antibacterial activity of TA-Cr<sub>2</sub>O<sub>3</sub> NCs

The well-diffusion method was performed to examine the bactericidal activity of *Acalypha indica* and *Carica papaya* plant extract synthesized chromium oxide-mediated tannic acid nanocomposite against *Pseudomonas* species, *Staphylococcus aureus*, *Escherichia coli* and *Enterococcus faecalis* (Figure 8). The synthesized TA-Cr<sub>2</sub>O<sub>3</sub> NC exhibits potent bactericidal activity against both the gram-positive and gram-negative bacteria. *Acalypha Indica* and *Carica papaya* plant extract were kept as the control. Compared to the control, *Pseudomonas* sp. is more susceptible to the TA-Cr<sub>2</sub>O<sub>3</sub> nanocomposite showing ZOI of 20 mm at 100 µg/ml. Followed by, *Escherichia coli* (14 mm), *Enterococcus faecalis* (13 mm), and *Staphylococcus*

aureus (12 mm) at 100  $\mu\text{g/mL}$ . In all tested bacteria, the activity was increased with increasing the dosage of TA- $\text{Cr}_2\text{O}_3$  NC was found to be 25 to 100  $\mu\text{g/mL}$  (Figure 7).

Figure 7. Graph representing ZOI of TA- $\text{Cr}_2\text{O}_3$  NCs

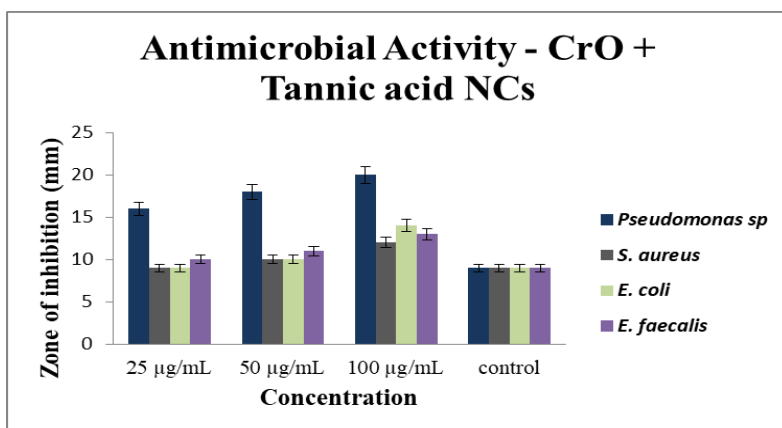
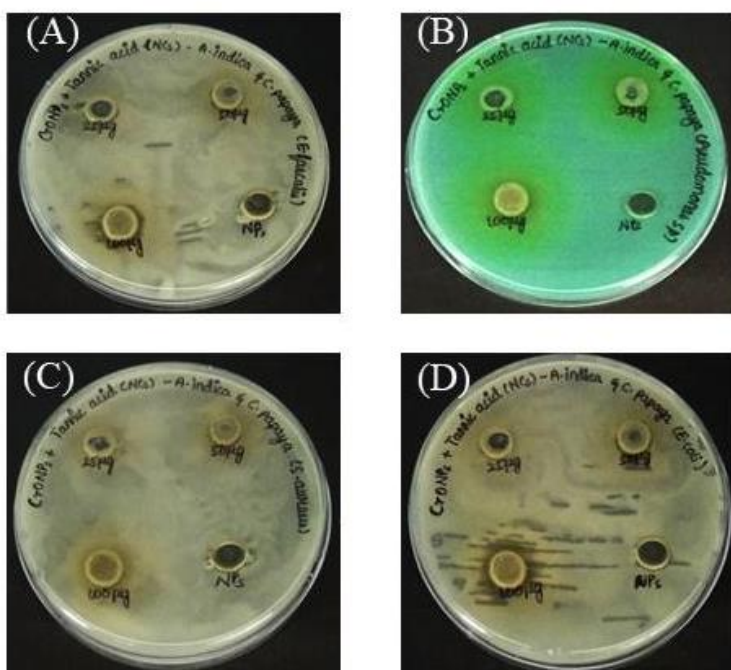


Figure 8. a) Enterococcus faecalis b) Pseudomonas sp. c) Staphylococcus aureus d) Escherichia coli

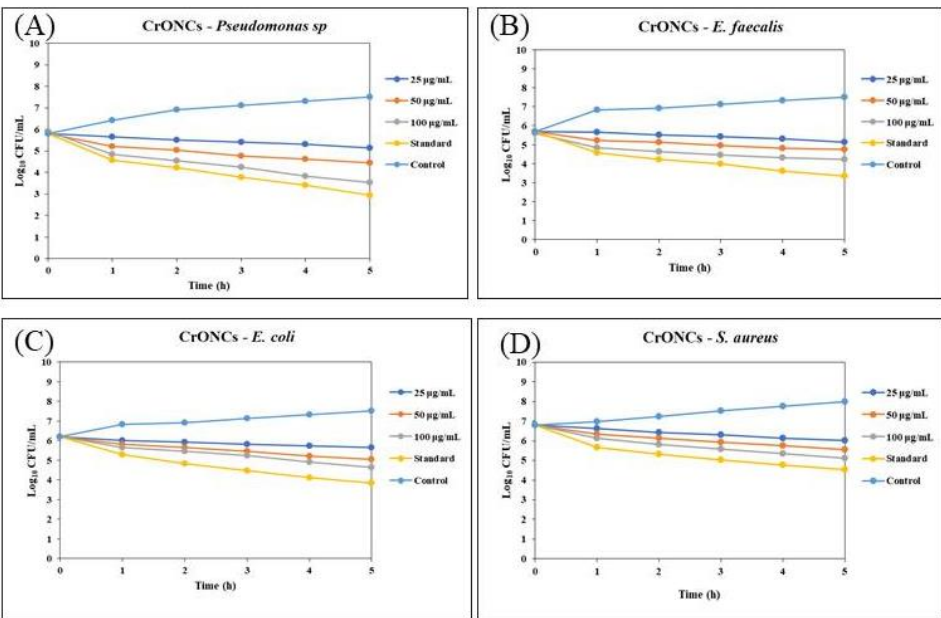


### 3.2.1. Time kill curve assay

This assay was used to evaluate bacterial growth and death and to observe the antibacterial inhibition effects with time. To investigate the antibacterial kinetics of TA- $\text{Cr}_2\text{O}_3$  nanocomposite, the current study conducted time-kill experiments using *Pseudomonas sp*,

*Staphylococcus aureus*, *Escherichia coli*, and *Enterococcus faecalis* as models for Gram-positive and Gram-negative bacteria, (Figure 9) respectively. It is considered a bactericidal agent if the antibacterial activity is  $\leq 3 \log_{10}$  in the CFU/ml. At the highest concentration of nanocomposites (100  $\mu\text{g/mL}$ ), after 5 hours *Pseudomonas* sp exhibited the bacteriostatic effect (6  $\log_{10}$  to 3.53  $\log_{10}$ ), *Escherichia faecalis* (5.6 to 4.23  $\log_{10}$ ), *Escherichia coli* (6.2 to 4.63  $\log_{10}$ ) and least microbial activity was obtained by *Staphylococcus aureus* (6.8 to 5.13  $\log_{10}$ ). The bacteriostatic effect was also seen in the lowest concentration (25  $\mu\text{g/mL}$ ) as well, for *Pseudomonas* sp (6  $\log_{10}$  to 5.14  $\log_{10}$ ), *E. coli* (6.2  $\log_{10}$  to 5.64  $\log_{10}$ ), *S. aureus* (6.8  $\log_{10}$  to 6.01  $\log_{10}$ ) and *E. faecalis* (5.6  $\log_{10}$  to 5.14  $\log_{10}$ ).

Figure 9. Graph representing time-kill curve assay of TA-Cr<sub>2</sub>O<sub>3</sub> nanocomposite. a) *Pseudomonas* sp b) *E. faecalis* c) *E. coli* d) *S. aureus*



### 3.3. Antioxidant activity of TA-Cr<sub>2</sub>O<sub>3</sub> NCs

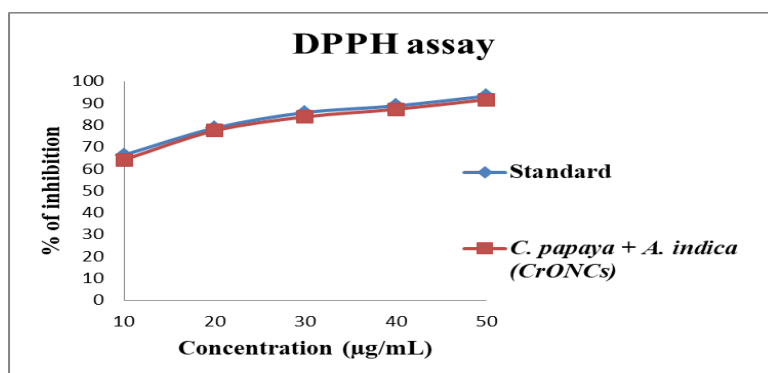
The antioxidant activity of biogenic fabricated tannic acid mediated chromium oxide nanocomposite (TA-Cr<sub>2</sub>O<sub>3</sub> NCs) was evaluated using multiple assays, including DPPH, H<sub>2</sub>O<sub>2</sub>, FRAP, ABTS, and Nitric oxide (NO). The biosynthesis of TA-Cr<sub>2</sub>O<sub>3</sub>NCs might lead to the absorption of numerous antioxidant compounds onto the active surface of nanoparticles. Due to the adsorbed antioxidant moiety onto the surface, the surface reaction phenomenon of these biosynthesized nanoparticles and the high surface area to volume ratio of nanoparticles create an inclination to interact and scavenge these free radicals.

#### 3.3.1. DPPH assay

DPPH has been widely used to test the radical scavenging activity of numerous chemicals and synthesized compounds. DPPH is a stable organic free radical compound and was based on the reduction of alcoholic DPPH solution in the presence of hydrogen-donating antioxidants. Figure 10, The tannic acid-mediated chromium oxide nanocomposite demonstrated a dose-

dependent scavenging effect on DPPH. With concentrations ranging from 10 to 50  $\mu\text{g/ml}$ , the DPPH scavenging potency of the TA- $\text{Cr}_2\text{O}_3$  nanocomposites increased from 64.09 % to 91.55 % of inhibition, whereas standard ascorbic acid showed a similar % of inhibition from 66.25 % to 93.15 %.

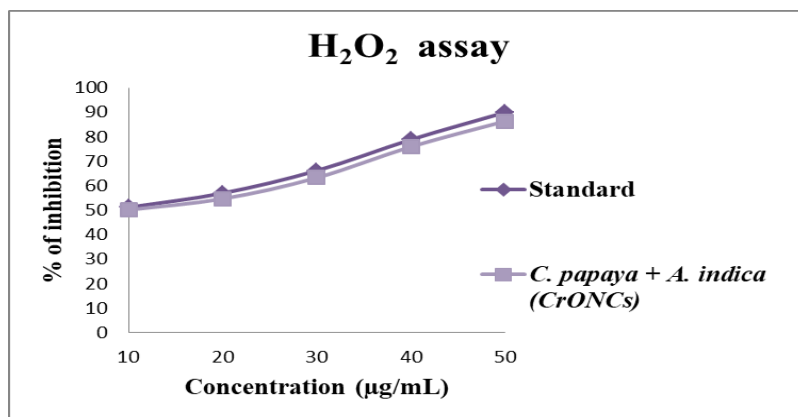
Figure 10. Graph representing DPPH assay of TA- $\text{Cr}_2\text{O}_3$  NCs



### 3.3.2. Hydrogen peroxide assay

The  $\text{H}_2\text{O}_2$  assay evaluates the ability of the plant extract to scavenge hydrogen peroxide, a harmful reactive oxygen species that can cause oxidative stress to cells and tissues. The assay (Figure 11) measures the reduction in hydrogen peroxide concentration after exposure to the nanoparticles, indicating antioxidant potential. The scavenging ability of *Acalypha indica* and *Carica papaya* mediated TA- $\text{Cr}_2\text{O}_3$  NCs and Ascorbic acid on hydrogen peroxide exhibited 50.1 to 86.3 % and 51.1 to 89.9 % which shows great antioxidant activity in 10 to 50  $\mu\text{g/mL}$  concentrations.

Figure 11. Graph representing  $\text{H}_2\text{O}_2$  assay of TA- $\text{Cr}_2\text{O}_3$  NCs

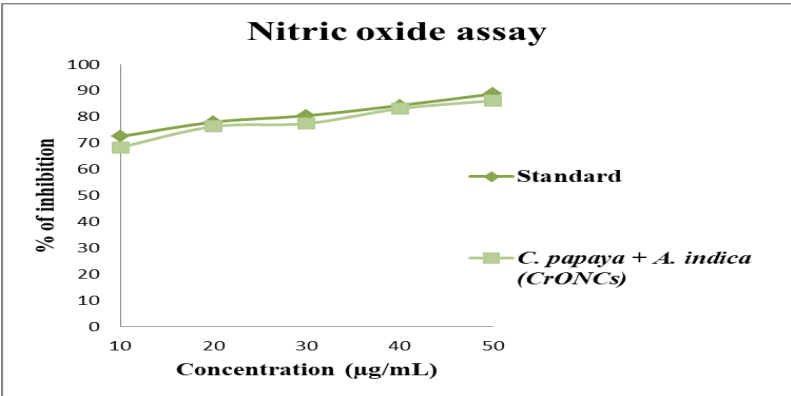


### 3.3.3. Nitric oxide assay

Nitric oxide (NO) participates in various biological processes such as relaxing smooth muscles, transmitting nerve signals, fighting against tumours, regulating blood pressure, and exhibiting antimicrobial activities. However, it also contributes to oxidative damage as it reacts

with superoxide to form the peroxynitrite anion, which can cause DNA fragmentation and initiate lipid peroxidation. Therefore, it is essential to regulate the production of nitric oxide carefully to prevent its harmful effects (Andrabi et al., 2023). The results of the nitric oxide radical scavenging assay done by Tannic acid-mediated chromium oxide nanocomposites show increased scavenging ability which ranges from 68.31 to 86.11 % of inhibition with the increase in the concentration of the TA-Cr<sub>2</sub>O<sub>3</sub> NCs sample. The standard ascorbic acid results from 72.43 % to 88.67 % (Figure 12). This indicates the good antioxidant activity of TA-Cr<sub>2</sub>O<sub>3</sub> NCs.

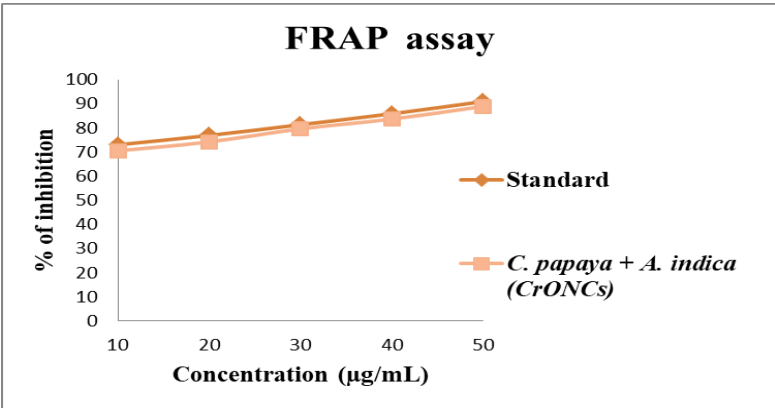
Figure 12. Graph representing NO assay of TA-Cr<sub>2</sub>O<sub>3</sub> NCs



3.3.4. FRAP assay

Figure 13, The FRAP assay is used to evaluate the ability of the antioxidant potential of samples by reducing ferric ions to ferrous ions through antioxidants present in the samples. Once the ferric iron is reduced, a blue colour is developed. The assay measures the reduction potential to estimate the antioxidant capacity of a sample. An increase in reduction potential indicates an increase in antioxidant activity. The scavenging effect of TA-Cr<sub>2</sub>O<sub>3</sub> nanocomposites was dependent on the dose. The FRAP assay potency of the TA-Cr<sub>2</sub>O<sub>3</sub> nanocomposites increased from 70.46 to 88.87% within the concentration range of 10 to 50 µg/ml. The standard ranges from 72.98 % to 90.89 %.

Figure 13. Graph representing FRAP assay of TA-Cr<sub>2</sub>O<sub>3</sub> NCs

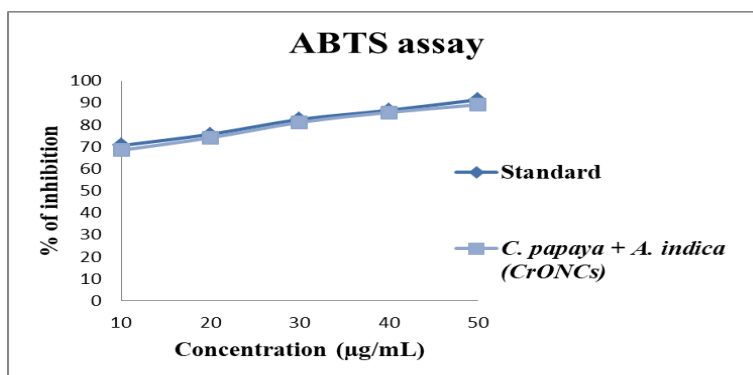




### 3.3.5. ABTS assay

The ABTS radical-scavenging measurement method, which is commonly used to evaluate antioxidant activity, takes advantage of the fact that ABTS free radicals become stable by accepting a hydrogen ion from the antioxidant, losing their blue colours. Moreover, ABTS radicals are produced from the oxidation of ABTS by potassium persulfate and it is an excellent tool for appraising the antioxidant potential of the hydrogen-donating and chain-breaking antioxidants. The standard ascorbic acid results from 70.56 % to 91.39 % inhibition. Herein the results observed are increased in the percentage of inhibition (68.42 to 89.07 %) with an increase in the dose concentration (10 to 50  $\mu\text{g/mL}$ ) (Figure 14).

Figure 14. Graph representing ABTS assay of TA-Cr<sub>2</sub>O<sub>3</sub> NCs

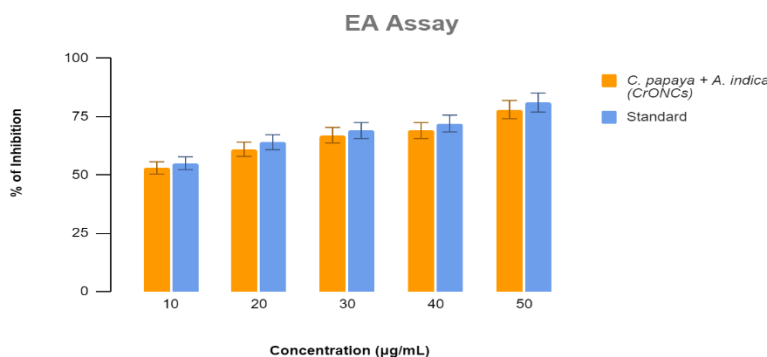


## 3.4. Anti-inflammatory activity

### 3.4.1. Egg albumin assay

The egg albumin denaturation assay is a method that aims to identify substances with anti-inflammatory properties. This method was based on the theory that such substances can stabilize protein structures and prevent denaturation. This experiment reveals the great anti-inflammatory properties of TA-Cr<sub>2</sub>O<sub>3</sub> NCs (Figure 15). Our findings revealed that TA-Cr<sub>2</sub>O<sub>3</sub> nanocomposites and standard Diclofenac were able to inhibit inflammation by 53% to 78% and 55% to 81%, depending on the concentration of the nanocomposites used.

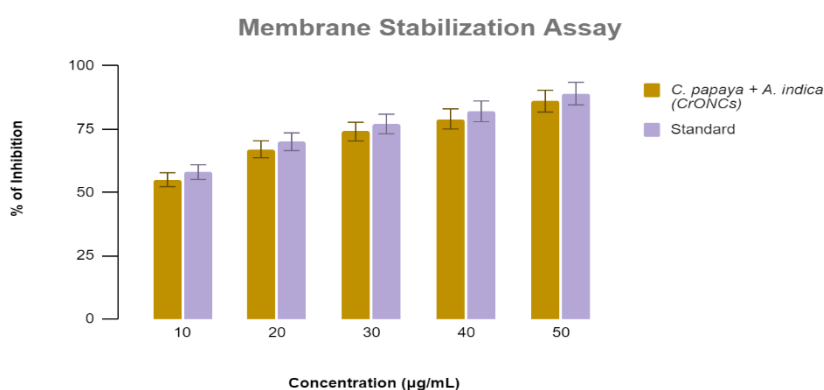
Figure 15. Graph representing Egg albumin assay of TA-Cr<sub>2</sub>O<sub>3</sub> NCs



### 3.4.2. Membrane stabilisation assay

The nanocomposites prepared from plant extracts of *Acalypha indica* and *Carica papaya* significantly protect the human blood erythrocyte membrane against lysis induced by hypotonic solution (Figure 16). At the concentration of 10-50  $\mu\text{g/mL}$ , a dose-dependent increase in the membrane stabilization was observed. The highest concentration of the sample (50  $\mu\text{g/mL}$ ) afforded 86% inhibition and at the lowest concentration (10  $\mu\text{g/mL}$ ) it exhibited 55% inhibition. The standard Diclofenac results show 58% to 89% inhibition. Thus, the observed results exhibit great anti-inflammatory activity for TA- $\text{Cr}_2\text{O}_3$  NC and can stabilize the cell membrane by preventing its disruption and subsequent release of intracellular contents.

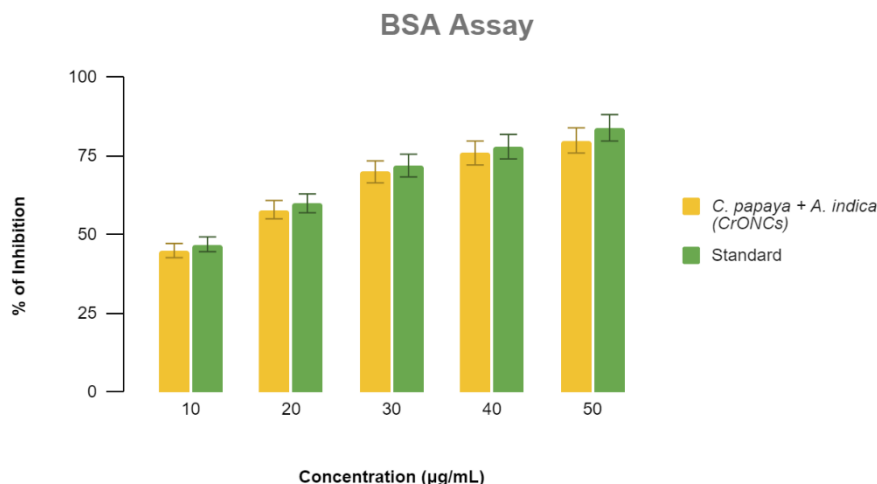
Figure 16. Graph representing Membrane stabilisation assay of TA- $\text{Cr}_2\text{O}_3$  NCs



### 3.4.3. Bovine serum assay

Citrus reticulata (Orange) peel was air-dried, crushed, and powdered. A Citrus reticulata peel powder weighing 1g of the powder was dissolved in 100 milliliters of distilled water. The mixture solution was then heated for 15 minutes at  $50^\circ\text{C}$ . After heating, the extract was filtered through a muslin cloth (Figure 1).

Bovine serum albumin (BSA), when subjected to heat, undergoes denaturation and initiates the expression of the antigen-associated response. The anti-denaturation assay is evaluated as a significant method for stabilizing compounds against allergies. In current research, we found that the TA- $\text{Cr}_2\text{O}_3$  nanocomposites have great anti-inflammatory properties. The findings revealed that the nanocomposites and standard were able to inhibit inflammation by 45 to 80% and 47 to 84%, depending on the concentration of the nanocomposites used (Figure 17).

Figure 17. Graph representing BSA assay of TA-Cr<sub>2</sub>O<sub>3</sub> NCs

### 3.5. Anticoagulant activity

The two blood samples (control & NCs) were observed for 1 hour at room temperature. The results show that TA-Cr<sub>2</sub>O<sub>3</sub> nanocomposites inhibited the formation of blood clots in the human blood samples even after 1-hour observation as shown in Figure 18. The control blood sample was clotted within 6 minutes. Hence proved that our biosynthesised tannic-acid mediated chromium oxide nanocomposites have anticoagulant activity and can be used as nanomedicine.

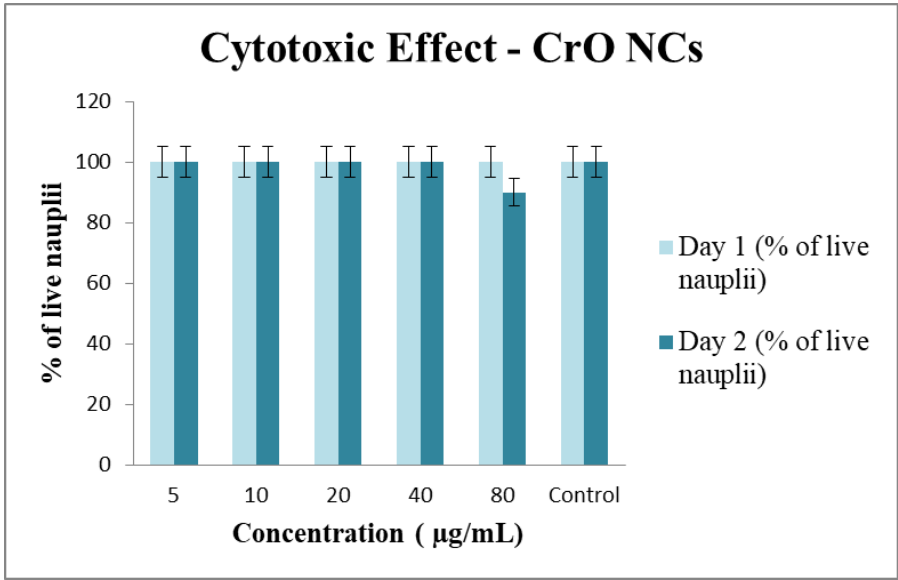
Figure 18. Control & TA-Cr<sub>2</sub>O<sub>3</sub> NC added to blood showing Anticoagulant activity

3.6. Cytotoxicity activity

3.6.1. Brine shrimp lethality assay

The test for cytotoxic properties was assessed using brine shrimps (Figure 19). With concentrations 5, 10, 20, 40, and 80  $\mu\text{g/ml}$  of TA- $\text{Cr}_2\text{O}_3$  nanocomposites sample, the results observed were 100% live nauplii with no lethal activity. This indicates that the prepared nanocomposites are not toxic to the cells of brine shrimp nauplii as they were all found to be alive on both days of observation except at higher concentrations (80  $\mu\text{g/ml}$ ) with a 90 % live rate on day 2.

Figure 19. Graph representing cytotoxicity of TA- $\text{Cr}_2\text{O}_3$  NCs



4. Discussion

Biologically reduced metal nanoparticles, such as chromium, iron, silver, and zinc oxides, are well-known for their multifunctional properties and biocompatibility enhancement.  $\text{Cr}_2\text{O}_3$  NPs, which are environmentally friendly and widely applicable, are multifunctional in nature. In this study, chromium oxide nanoparticles were prepared using the leaf extract of *Acalypha indica* and *Carica papaya*, and then the prepared nanoparticles were treated with tannic acid, a natural antioxidant, to explore their various nanomedicinal applications. The extracts of plants contain bioactive chemical compounds that can catalyze redox reactions and act as stabilizing and capping agents. Phenols, terpenoids, flavones, tannic acid, and other enzymes, as well as carbohydrates like phytochemicals, can act as reducing and stabilizing agents. This study reported the SPR peak of TA- $\text{Cr}_2\text{O}_3$  NPs at 410 nm after 48 hours at UV-vis spectra. Similar absorbance peaks were observed in an article, where  $\text{Cr}_2\text{O}_3$  NPs were synthesised by the reduction route method using trioctylphosphine oxide (TOPO) showing peaks at 415 nm, 590 and 690 nm (Babukutty et al., 2015). Phyto-fabricated  $\text{Cr}_2\text{O}_3$  NPs using *Hyphaene thebaica* reveal a SPR resonance peak at approximately 350 nm (Mohamed et al., 2020). This study is

the first to mediate tannic acid with chromium oxide nanoparticles which makes it a nanocomposite with an SPR peak of 360 nm. The synthesized chitosan-based nanocomposite using tannic acid and showed quite similar absorbance at 280 nm (Roy et al., 2021). Biogenic  $\text{Cr}_2\text{O}_3$  NPs revealed more potent antibacterial properties than other synthesis methods and have a strong role in disrupting the microbial cell organelles which leads to cell prefoliation destruction (Nguyen & Bhattacharya, 2022). A recent study investigated  $\text{Cr}_2\text{O}_3$  NPs biosynthesised from *Phyllanthus emblica* which revealed great antibacterial properties with the maximum zone of inhibition seen against *A. baumannii* and when compared to our results higher ZOI is seen in *Pseudomonas*, *E. coli* and *S. aureus* species (Fatima et al., 2024). Single route precursor and cinnamon bark synthesised  $\text{Cr}_2\text{O}_3$  NPs exhibited excellent antibacterial properties against *E. coli* (25 mm), *B. subtilis* (20 mm), and *P. aeruginosa* (27 mm) which shows higher activity than our results (Kothari & Soni, 2022). Studies conducted with  $\text{Cr}_2\text{O}_3$  NPs prepared from *Nigella sativa* seed extract tested against *Staphylococcus aureus*, *Klebsiella pneumonia* and *Pseudomonas aeruginosa* showing ZOI 16 mm, 25 mm and 15 mm which show similar activity with TA- $\text{Cr}_2\text{O}_3$  NC (Duraivathi et al., 2022). A recent study synthesized chromium oxide NPs from *M.charantia*, revealed a lower Zone of inhibition compared to our results (David et al., 2023).  $\text{Cr}_2\text{O}_3$  NPs prepared using natural honey which shows great antibacterial activity with ZOI of 15 mm and 10 mm for *Staphylococcus aureus* and *Escherichia coli* (Nivethitha & Rachel, 2022). In the article, phyto fabricated  $\text{Cr}_2\text{O}_3$  NPs revealed dose-dependent antibacterial properties. *Escherichia coli* showed the highest ZOI (18 mm) at lower concentrations (4 mg/ml). Furthermore, a good antioxidant nature was obtained in multiple assays for TA- $\text{Cr}_2\text{O}_3$  NPs (Mohamed et al., 2020). Results obtained are compared to a similar article that investigated DPPH radicals scavenging using *Rhamnus virgata*-mediated  $\text{Cr}_2\text{O}_3$  NPs that showed significant inhibit ion (79.56 %) in the highest dose concentration (Iqbal et al., 2020). A bioinspired  $\alpha\text{-Cr}_2\text{O}_3$  NPs were tested for antioxidant properties which showed the highest scavenging at  $57.69 \pm 2.19$  obtained at 200  $\mu\text{g/ml}$  (Hassan et al., 2019). Bimetallic nanoparticles made with chromium and other metal nanoparticles more efficiently inhibit bacterial strains than metallic nanoparticles.  $\text{TiO}_2@\text{Cr}_2\text{O}_3$  NPs were tested for antibacterial activity with several bacterial strains such as *S. aureus*, *B. subtilis*, *P. aeruginosa*, *E. coli*, *C. albicans* and *A. niger*. All bacterial strains show 100% inhibition at 100  $\mu\text{g/ml}$  (Hasanin et al., 2023). Furthermore, synthetic AgCr Nps have also been revealed to have potential antibacterial effects on *S. aureus*, *E. coli* and *E. faecalis* (Abirami et al., 2023). The study reveals the highest DPPH radical scavenging properties at 84.12% at 60 mins (Cheah et al., 2023). A good to moderate antioxidant potential of  $\text{Cr}_2\text{O}_3$  NPs was recorded in the article where DPPH free radical scavenging potential ranged between 49.47 and 23.65 % (Mohamed et al., 2020). Using a similar procedure, *C. viminalis* bio-reduced  $\text{Cr}_2\text{O}_3$  NPs revealed a slightly higher antioxidant activity. Similar results have been found in a recent article, which shows significant antioxidant activity using hydrogen peroxide assay in the range of 43.56% to 82.64% (Ahmad et al., 2023). Tannic acid crosslinked and  $\text{TiO}_2$ -reinforced chitosan nanocomposite films are biosynthesised to evaluate their antioxidant properties using DPPH and ABTS radical scavenging assays and obtained results of 42.4% and 64.5% respectively (Roy et al., 2021). The biocidal properties of  $\text{Cr}_2\text{O}_3$  nanoparticles can be explained by their interactions with cells on a mechanistic level. The small size of the nanoparticles enables them to penetrate cells easily and produce reactive oxygen species (ROS), which causes oxidative stress and ultimately leads to cell death. Furthermore, the ROS produced can

interact with cellular machinery, enzymes, and organelles in addition to the nanoparticles (Čapek & Roušar, 2021). Findings revealed good antioxidant and anti-inflammatory properties of Cr<sub>2</sub>O<sub>3</sub> NPs with 43% and 44% inhibition at 200 µg/ml and 800 µg/ml concentrations which shows good results when compared to our results (Roy et al., 2021). Chromium picolinate-mediated Zinc nanoparticles were tested for cytotoxic properties in which a lethal dose (LD50) concentration was obtained to be 15 µL with half the population of nauplii surviving after post-incubation (Shree et al., 2020). As compared to a study that assesses the cytotoxicity of Cr<sub>2</sub>O<sub>3</sub> NPs using an In-vitro brain shrimp lethality assay. It was observed that 100% mortalities were witnessed when the highest dose of 400 µg/ml was used. However, the mortality of the shrimps decreased to 40% when the treatment dosage was reduced to 12.5 µg/ml (Mohamed et al., 2020).

## 5. Conclusion

Bioreduction of metal nanoparticles using plant extracts is a novel route for assembling metal nanoparticles with multifunctional properties. Tannic acid-mediated Chromium oxide nanocomposite was synthesized by leaf extracts of *Acalypha indica* and *Carica papaya* as a bio-reducing and stabilizing agent. Characterisation UV-visible spectra and X-ray diffraction (XRD) are used to analyze their structural properties. The prepared nanocomposites indicated a significant bactericidal effect and potential time-kill curve assay. The potent free radical scavenging potential was obtained using multiple antioxidant assays. TA-Cr<sub>2</sub>O<sub>3</sub> NCs were tested for anti-inflammatory properties which shows great potential. TA-Cr<sub>2</sub>O<sub>3</sub> NCs also revealed effective cytotoxic effects against the brine shrimp lethality test. Our results indicate a dose-responsive bioactivity of TA-Cr<sub>2</sub>O<sub>3</sub> NCs. Overall, the multifunctional nature of the tannic acid-mediated chromium oxide nanoparticles synthesized from *Acalypha indica* and *Carica papaya* is concluded.

### Funding Details

No funding was acquired for carrying out this study.

### Disclosure Statement

The authors declare that they have no known competing financial interests or personal relationships that could have appeared to influence the work reported in this paper.

## References

1. Abirami, P., Sampath, S., Al-Ansari, M. M., Al-Dahmash, N. D., Lopes, B. S., Vincent, S., & Saravanan, M. (2023). One-pot synthesis of Ag-Cr bimetallic nanoparticles from *Catharanthus roseus* for anti-bacterial, anticancer, anti-diabetic, and anti-inflammatory activity and toxicity study in zebrafish. *Biomass Conversion and Biorefinery*. <https://doi.org/10.1007/s13399-023-04767-9>
2. Ahmad, T. (2014). Reviewing the Tannic Acid Mediated Synthesis of Metal Nanoparticles. *Journal of Nanotechnology*, 2014, 1–11. <https://doi.org/10.1155/2014/954206>
3. Ahmad, W., Joshi, A., Kumar, S., Rana, R., & Arora, A. (2023). Bio-extract-mediated microwave-assisted synthesis of Cr<sub>2</sub>O<sub>3</sub> nanoparticles: Characterization, antibacterial,



- antioxidant, and photocatalytic activity evaluation. *MRS Advances*.  
<https://doi.org/10.1557/s43580-023-00715-x>
4. Andrabi, S. M., Sharma, N. S., Karan, A., Shahriar, S. M. S., Cordon, B., Ma, B., & Xie, J. (2023). Nitric Oxide: Physiological Functions, Delivery, and Biomedical Applications. *Advanced Science*, 10(30). <https://doi.org/10.1002/advs.202303259>
5. Azizi, A. (2020). Green Synthesis of Fe<sub>3</sub>O<sub>4</sub> Nanoparticles and Its Application in Preparation of Fe<sub>3</sub>O<sub>4</sub>/Cellulose Magnetic Nanocomposite: A Suitable Proposal for Drug Delivery Systems. *Journal of Inorganic and Organometallic Polymers and Materials*, 30(9), 3552–3561. <https://doi.org/10.1007/s10904-020-01500-1>
6. Babukutty, B., Parakkal, F., Bhalero, G. M., Aravind, P. B., & Nair, S. S. (2015). Structural, morphological and optical properties of chromium oxide nanoparticles. *AIP Conference Proceedings*. <https://doi.org/10.1063/1.4917789>
7. Bahrulolum, H., Nooraei, S., Javanshir, N., Tarrahimofrad, H., Mirbagheri, V. S., Easton, A. J., & Ahmadian, G. (2021). Green synthesis of metal nanoparticles using microorganisms and their application in the agrifood sector. *Journal of Nanobiotechnology*, 19(1). <https://doi.org/10.1186/s12951-021-00834-3>
8. Baldwin, A., & Booth, B. W. (2022). Biomedical applications of tannic acid. *Journal of Biomaterials Applications*, 36(8), 1503–1523. <https://doi.org/10.1177/08853282211058099>
9. Čapek, J., & Roušar, T. (2021). Detection of Oxidative Stress Induced by Nanomaterials in Cells—The Roles of Reactive Oxygen Species and Glutathione. *Molecules/Molecules Online/Molecules Annual*, 26(16), 4710. <https://doi.org/10.3390/molecules26164710>
10. Çetin, K., Denizli, F., Yavuz, H., Türkmen, D., & Denizli, A. (2019). Magnetic Nanoparticles and Their Biomedical Applications. *Hacettepe Journal of Biology and Chemistry*, 47(2), 143–152. <https://doi.org/10.15671/hjbc.622644>
11. Cheah, S. Y., Tey, L. H., Aminuzzaman, M., Phang, Y. K., Chan, Y. B., Djearmane, S., Wong, L. S., & Watanabe, A. (2023). Green Synthesis and Characterizations of Chromium Oxide Nanoparticles (Cr<sub>2</sub>O<sub>3</sub> NPs) Derived from Pomegranate Husk and its  $\alpha$ -Amylase Inhibitory and Antioxidant Properties. *Nano Hybrids and Composites*, 39, 51–55. <https://doi.org/10.4028/p-od359h>
12. David, S. A., Doss, A., & Pole, R. P. (2023). Biosynthesis of chromium oxide nanoparticles by *Momordica charantia* leaf extract: Characterization and their Antibacterial Activities. *Results in Surfaces and Interfaces*, 11, 100120. <https://doi.org/10.1016/j.rsufi.2023.100120>
13. Duraivathi, C., Jeya, J. P., Poongodi, J., & Johnson, H. J. (2022). GREEN SYNTHESIS OF CHROMIUM OXIDE NANOPARTICLES - STUDY OF ITS ANTIBACTERIAL, PHOTOCATALYTIC AND THERMODYNAMIC PROPERTIES. *Journal of Advanced Scientific Research*, 13(09), 17–23. <https://doi.org/10.55218/jasr.202213904>
14. Fatima, E., Arooj, I., Javeed, M., & Yin, J. (2024). Green synthesis, characterization and applications of *Phyllanthus emblica* fruit extract mediated chromium oxide nanoparticles. *Discover Nano*, 19(1). <https://doi.org/10.1186/s11671-024-04006-8>
15. Ghotekar, S., Pansambal, S., Bilal, M., Pingale, S. S., & Oza, R. (2021). Environmentally friendly synthesis of Cr<sub>2</sub>O<sub>3</sub> nanoparticles: Characterization, applications and future perspective — a review. *Case Studies in Chemical and Environmental Engineering*, 3, 100089. <https://doi.org/10.1016/j.csee.2021.100089>
16. Girija, D. M., Kalachaveedu, M., Rao, S. R., & Subbarayan, R. (2018). Transdifferentiation of human gingival mesenchymal stem cells into functional keratinocytes by *Acalypha indica* in three-dimensional microenvironment. *Journal of Cellular Physiology*, 233(11), 8450–8457. <https://doi.org/10.1002/jcp.26807>
17. Hasanin, M. S., Elhenawy, Y., Abdel-Hamid, S. M. S., Fouad, Y., Monica, T., Al-Qabandi, O. A., Fray, M. E., & Bassyouni, M. (2023). New Eco-Friendly, Biocompatible, Bactericidal, Fungicidal and Anticancer-Activity-Exhibiting Nanocomposites Based on Bimetallic

- TiO<sub>2</sub>@Cr<sub>2</sub>O<sub>3</sub> Nanoparticle Core and Biopolymer Shells. *Journal of Composites Science*, 7(10), 426. <https://doi.org/10.3390/jcs7100426>
18. Hassan, D., Khalil, A. T., Solangi, A. R., El-Mallul, A., Shinwari, Z. K., & Maaza, M. (2019). Physiochemical properties and novel biological applications of Callistemon viminalis-mediated  $\alpha$ -Cr<sub>2</sub>O<sub>3</sub> nanoparticles. *Applied Organometallic Chemistry*, 33(8). <https://doi.org/10.1002/aoc.5041>
  19. Iqbal, J., Abbasi, B. A., Munir, A., Uddin, S., Kanwal, S., & Mahmood, T. (2020). Facile green synthesis approach for the production of chromium oxide nanoparticles and their different in vitro biological activities. *Microscopy Research and Technique*, 83(6), 706–719. <https://doi.org/10.1002/jemt.23460>
  20. Isacfranklin, M., Ameen, F., Ravi, G., Yuvakkumar, R., Hong, S., Velaauthapillai, D., Thambidurai, M., & Dang, C. (2020). Single-phase Cr<sub>2</sub>O<sub>3</sub> nanoparticles for biomedical applications. *Ceramics International*, 46(12), 19890–19895. <https://doi.org/10.1016/j.ceramint.2020.05.050>
  21. Kanniah, P., Radhamani, J., Chelliah, P., Muthusamy, N., Balasingh, E. J. J. S., Thangapandi, J. R., Balakrishnan, S., & Shanmugam, R. (2020). Green Synthesis of Multifaceted Silver Nanoparticles Using the Flower Extract of *Aerva lanata* and Evaluation of Its Biological and Environmental Applications. *ChemistrySelect*, 5(7), 2322–2331. <https://doi.org/10.1002/slct.201903228>
  22. Kothari, R., & Soni, A. (2022). GREEN SYNTHESIS OF CHROMIUM OXIDE NANOPARTICLES USING CHROMIUM (III) COMPLEX AS A SINGLE ROUTE PRECURSOR: ANTI-OXIDANT ACTIVITY. *Rasayan Journal of Chemistry/Rasayan Journal of Chemistry*, 15(02), 1325–1339. <https://doi.org/10.31788/rjc.2022.1526700>
  23. Krishna, K. L., Paridhavi, M., & Patel, J. A. (2008). Review on nutritional, medicinal and pharmacological properties of Papaya (*Carica papaya* Linn.). <http://nopr.niscair.res.in/bitstream/123456789/5695/1/NPR%207%284%29%20364-373.pdf>
  24. Leader, B., Baca, Q. J., & Golan, D. E. (2008). Protein therapeutics: a summary and pharmacological classification. *Nature Reviews. Drug Discover/Nature Reviews. Drug Discovery*, 7(1), 21–39. <https://doi.org/10.1038/nrd2399>
  25. Mohamed, H. E. A., Afridi, S., Khalil, A. T., Zohra, T., Ali, M., Alam, M. M., Ikram, A., Shinwari, Z. K., & Maaza, M. (2020). Phyto-fabricated Cr<sub>2</sub>O<sub>3</sub> nanoparticle for multifunctional biomedical applications. *Nanomedicine*, 15(17), 1653–1669. <https://doi.org/10.2217/nnm-2020-0129>
  26. Mori, K., Naka, K., Masuda, S., Miyawaki, K., & Yamashita, H. (2017). Palladium Copper Chromium Ternary Nanoparticles Constructed In situ within a Basic Resin: Enhanced Activity in the Dehydrogenation of Formic Acid. *ChemCatChem*, 9(18), 3456–3462. <https://doi.org/10.1002/cctc.201700595>
  27. Naik, R., Nemani, H., Pothani, S., Pothana, S., Satyavani, M., Qadri, S. S., Srinivas, M., & Parim, B. (2019). Obesity-alleviating capabilities of *Acalypha indica*, *Pergularia ademia* and *Tinospora cardifolia* leaves methanolic extracts in WNIN/GR-Ob rats. *Journal of Nutrition & Intermediary Metabolism*, 16, 100090. <https://doi.org/10.1016/j.jnim.2019.02.001>
  28. Nguyen, T. L. A., & Bhattacharya, D. (2022). Antimicrobial Activity of Quercetin: An Approach to Its Mechanistic Principle. *Molecules/Molecules Online/Molecules Annual*, 27(8), 2494. <https://doi.org/10.3390/molecules27082494>
  29. Nivethitha, P. R., & Rachel, D. C. J. (2022). A study of antioxidant and antibacterial activity using honey mediated Chromium oxide nanoparticles and its characterization. *Materials Today Proceedings*, 48, 276–281. <https://doi.org/10.1016/j.matpr.2020.07.187>
  30. Perera, B., & Teklani, P. (2016). The important biological activities and phytochemistry of *Acalypha indica*. *International Journal of Research in Pharmacy and Science*, 1–1, 30–35. <http://www.ijrpsonline.com/pdf/6005.pdf>

31. Roy, S., Zhai, L., Kim, H. C., Pham, D. H., Alrobei, H., & Kim, J. (2021). Tannic-Acid-Cross-Linked and TiO<sub>2</sub>-Nanoparticle-Reinforced Chitosan-Based Nanocomposite Film. *Polymers*, 13(2), 228. <https://doi.org/10.3390/polym13020228>
32. Sahu, T., Ratre, Y. K., Chauhan, S., Bhaskar, L., Nair, M. P., & Verma, H. K. (2021). Nanotechnology based drug delivery system: Current strategies and emerging therapeutic potential for medical science. *Journal of Drug Delivery Science and Technology*, 63, 102487. <https://doi.org/10.1016/j.jddst.2021.102487>
33. Saran, P. L., & Choudhary, R. (2013). Drug bioavailability and traditional medicaments of commercially available papaya: A review. *African Journal of Agricultural Research*, 8(25), 3216–3223. <https://doi.org/10.5897/ajar2013.7295>
34. Shabatina, T. I., Vernaya, O. I., Shabatin, V. P., & Melnikov, M. Y. (2020). Magnetic Nanoparticles for Biomedical Purposes: Modern Trends and Prospects. *Magnetochemistry*, 6(3), 30. <https://doi.org/10.3390/magnetochemistry6030030>
35. Shree, M. K., Arivarasu, L., & Rajeshkumar, S. (2020). Cytotoxicity and Antimicrobial Activity of Chromium Picolinate Mediated Zinc Oxide Nanoparticle. *Journal of Pharmaceutical Research International*, 28–32. <https://doi.org/10.9734/jpri/2020/v32i2030726>
36. Singh, S. P., Kumar, S., Mathan, S. V., Tomar, M. S., Singh, R. K., Verma, P. K., Kumar, A., Kumar, S., Singh, R. P., & Acharya, A. (2020). Therapeutic application of Carica papaya leaf extract in the management of human diseases. *Daru*, 28(2), 735–744. <https://doi.org/10.1007/s40199-020-00348-7>
37. Wall, M. M. (2006). Ascorbic acid, vitamin A, and mineral composition of banana (*Musa* sp.) and papaya (*Carica papaya*) cultivars grown in Hawaii. *Journal of Food Composition and Analysis*, 19(5), 434–445. <https://doi.org/10.1016/j.jfca.2006.01.002>
38. Wang, D., Zhang, S., Chang, Z., Kong, D. X., & Zuo, Z. (2017). Quebrachitol: Global Status and Basic Research. *Natural Products and Bioprospecting*, 7(1), 113–122. <https://doi.org/10.1007/s13659-017-0120-3>
39. Yemmen, M., Landolsi, A., Hamida, J. B., Mégraud, F., & Ayadi, M. T. (2017). Antioxidant activities, anticancer activity and polyphenolics profile, of leaf, fruit and stem extracts of *Pistacia lentiscus* from Tunisia. *Cellular and Molecular Biology*, 63(9), 87–95. <https://doi.org/10.14715/cmb/2017.63.9.16>
40. Ying, S., Guan, Z., Ofoegbu, P. C., Clubb, P., Rico, C., He, F., & Hong, J. (2022). Green synthesis of nanoparticles: Current developments and limitations. *Environmental Technology & Innovation*, 26, 102336. <https://doi.org/10.1016/j.eti.2022.102336>
41. Zainab, N., Ahmad, S., Khan, I., Saeed, K., Ahmad, H., Alam, A., Almeahmadi, M., Alsaiani, A. A., Haitao, Y., & Ahmad, M. (2022). A study on green synthesis, characterization of chromium oxide nanoparticles and their enzyme inhibitory potential. *Frontiers in Pharmacology*, 13. <https://doi.org/10.3389/fphar.2022.1008182>
42. Zelekew, O. A., Fufa, P. A., Sabir, F. K., & Duma, A. D. (2021). Water hyacinth plant extract mediated green synthesis of Cr<sub>2</sub>O<sub>3</sub>/Zn composite photocatalyst for the degradation of organic dye. *Heliyon*, 7(7), e07652. <https://doi.org/10.1016/j.heliyon.2021.e07652>
43. Zhu, G. N., Wang, Y. G., & Xia, Y. Y. (2012). Ti-based compounds as anode materials for Li-ion batteries. *Energy & Environmental Science*, 5(5), 6652. <https://doi.org/10.1039/c2ee03410g>